Magazine of Civil Engineering

ISSN 2071-0305

journal homepage: http://engstroy.spbstu.ru/

DOI: 10.18720/MCE.96.7

Impact of anchored CFRP on the torsional and bending behaviour of RC beams

R. Al-Rousan*, I. Abo-Msamh
Jordan University of Science and Technology, Irbid, Jordan

** E-mail: rzalrousan@just.edu.jo*

Keywords: reinforced concrete, structural strength, structural models, bonding, torsion, flexural strength, fiber reinforced polymer

Abstract. The scientific problem considered in the study is indeed one of the problems in the modern theory of reinforced concrete. Despite a significant number of studies on the problem of bending with torsion, to date. There are no sufficiently reliable solutions to this problem that most fully reflect the physical nature of the problem. In the last two decades, using of Carbon Fiber Reinforced Polymers (CFRP) in strengthening of deficient reinforced concrete structural elements has been increased due to their ease of installation, low invasiveness, high corrosion resistance, and high strength to weight ratio. Strengthening damage structures is a relatively new technique. Therefore, the intent was to appear at the essential CFRP external strengthening technique that provides an efficient increase in the shear and flexural strengths as maintaining ductile failure mode. However, anchoring and debonding problems remains a challenge for the accomplishment of this technique. In this study, a novel application was implemented in which the CFRP sheet was integrated as external shear strengthening for RC beams. Therefore, this study investigated the behavior of simply supported RC beams strengthened externally with anchored CFRP composite using and subjected to combined bending and torsion using Nonlinear Finite Element Analysis (NLFEA). Seventeen models have been constructed and divided into four groups to scrutinize the effect of CFRP anchored depth and CFRP strip spacing. The performance of each beam was evaluated in terms of failure mode, CFRP strain, load-deflection and torsion-twist behavior, ultimate deflection, ultimate load capacity, ultimate angle of twist, ultimate torsion capacity, elastic stiffness, and energy absorption. The enhancement percentage increased with the increase of anchored depth and decreased with the increase of CFRP strip spacing. Finally, the external strengthening with anchored had a superior effect on the ultimate load, ultimate deflection, angle of twist, torsion elastic stiffness, energy absorption.

1. Introduction

In recent decades, repair and strengthening of reinforced concrete (RC) buildings and bridges have become increasingly common. Deficiencies in RC members may exist for several reasons, including changes in use of the structure, design and constructions errors, and degradation due to environmental conditions [1–4]. RC members are commonly strengthened in flexure, shear, and/or confinement depending on the member loading conditions and type of enhancement needed [5–7]. In some cases, RC members are subjected to significant torsional moments, and the torsional strength needs to be enhanced. Accordingly, methods and design provisions for strengthening RC members in torsion are needed.

The Reinforced Concrete (RC) structural elements such as the peripheral beams in each floor of multi-storied buildings, ring beams at the bottom of circular tanks, edge beams of shell roofs, the beams supporting canopy slabs and the helical staircases are subjected to significant torsional loading in addition to flexure and shear. In reinforced concrete design, depending on the load transfer mechanism the torsion is classified as 'equilibrium torsion' and 'compatibility torsion'. Equilibrium torsion is induced in beams supporting lateral overhanging projections, and is caused by the eccentricity in the loading. In compatibility torsion, torsion is induced in a structural member by rotations (twists) applied at one or more points along the length of the member. The twisting moments induced are generally statically indeterminate and their analysis necessarily involves compatibility conditions. Hence it is named 'compatibility torsion'. The structural elements subjected to torsion show cracking if they are not designed and detailed properly. Further, change in loading or

Al-Rousan, R., Abo-Msamh, I. Impact of anchored CFRP on the torsional and bending behaviour of RC beams. Magazine of Civil Engineering. 2020. 96(4). Pp. 79–93. DOI: 10.18720/MCE.96.7

deterioration of structural element cause the deficiency in torsional resistance. Also, in recent past earthquakes, it has been seen that structures showed failure and some have been severely damaged. Such disasters have demonstrated the need for retrofitting of seismically deficient structures. Retrofitting allows strengthening of elements to resist the strength demands predicted by the analysis, without significantly affecting the overall response of the structure.

The fiber reinforced polymer (FRP) has been proved to be a widely used strengthening material for deficient RC members. It has various well-known advantages such as high strength to weight ratio, high corrosive resistance, and easy-to-apply character. Many significant experimental and theoretical studies in the past have been carried out to understand the flexural [1, 2] and shear [3, 4] behaviors of RC members externally strengthened with FRP materials since the bending moments and shear forces are regarded as primary effects, whereas the torsional strengthening has not been studied in much depth, which was just initiated in 2001 [8–10]. Torsion can be considered as primary effect, however, in some special situations such as spandrel or curved beams, eccentrically loaded bridge girders, and bridge columns under seismic load. In this case, it is important to conduct deep researches on the torsional behavior of RC members strengthened with FRP materials, including experimental, numerical and analytical investigations.

Most of the test specimens in previous experimental investigations were solid rectangular RC beams externally strengthened with carbon or glass FRP (CFRP or GFRP) materials under monotonic torsion [11–13]. Few tests of RC box beams strengthened with CFRP sheets have been conducted under monotonic torsion [14] and under cyclic torque [15]. To understand the influence of strengthening schemes of FRP system on the effectiveness of upgrading in torsional resistance of RC members [16–23], the various FRP wrapping configurations have been investigated by considering the fiber orientation, the number of beam faces strengthened, the effect of number of FRP plies used, and the influence of anchors in U-wrapped test beams [16, 17]. The results have showed that the 45 spiral wrap is a much more efficient torsional strengthening scheme than vertical strips. Few researches on non-rectangular beams have been carried out in recent years. RC T-beams strengthened with different strengthening techniques under pure torsion [16] and combined shear and torsion [17] have been investigated. Spandrel RC beams strengthened with CFRP laminates also have been tested under torsion [18]. In addition, the torsional repair of damaged rectangular [19] and circular [20] RC columns with FRP materials, which helps to enhance the ultimate rotational strength, has been carried out in recent years.

Owing to the fact that experimental investigation costs much time and money, the finite element analysis (FEA) using commercial software is a beneficial supplement to the study of torsional behavior. Numerical studies on the cracking and crushing patterns [12], the damage simulation [24], the effect of CFRP and reinforcing steel bars on the contribution to the torsional behavior [10], and the torque–twist curves [23] of RC beams were performed through FEA softwares, such as ANSYS, ABAQUS, DIANA, Algor SAP and so on [25-29]. Therefore, essential issues to produce effective, economical, and successful CFRP strengthening were discussed. Also, the impact of anchored CFRP external strengthening on the behavior of reinforced concrete beams subjected to bending and torsion received miniature consideration. The scientific problem considered in the study is indeed one of the problems in the modern theory of reinforced concrete. Despite a significant number of studies on the problem of bending with torsion, to date. There are no sufficiently reliable solutions to this problem that most fully reflect the physical nature of the problem. In this study, a novel application was implemented in which the CFRP sheet was integrated as external shear strengthening for RC beams. A lack of literature regarding the behavior of simply supported RC beams strengthened externally with CFRP composite and subjected to combined bending and torsion are necessitated conducting the present investigation. The main objectives of this study are to predict the bending and torsion of RC beams strengthened externally with anchored CFRP composite using Nonlinear Finite Element Analysis (NLFEA) taking into account the effects of four major strengthening configuration including: 1) One layer of 50 mm U strip wrapping at 225 mm c/c with an additional layer of CFRP wrapping on both sides of the web; 2) One layer of 50 mm U strip wrapping at 175 mm c/c with an additional layer of CFRP wrapping on both sides of the web; 3)One layer of 50 mm U strip wrapping at 125 mm c/c with an additional layer of CFRP wrapping on both sides of the web; and 4)One layer of 50 mm U strip wrapping at 75 mm c/c with an additional layer of CFRP wrapping on both sides of the web. As a result, seventeen models have been constructed and subjected to combined bending and torsion. For this purpose, validation against the previous experimental study reported by Gesund et al. [30] is firstly simulated using ANSYS software. After that, a parametric study is extended for strengthened RC beams using different configurations of CFRP.

2. Methods

ANSYS software is a numerical method used to simplify the analysis of a variety of engineering problems. To reduce the complexity of load setup, effort, time and cost during the experimental testing, ANSYS software had been used by many researchers. It was recommended about this software to be used since their results achieved good agreement with experimental results. ANSYS is general-purpose software used in this study. Twenty-six full-scale models strengthened using CFRP are developed to carry out different investigated parameters.

2.1. Experimental Work Review

The validation process of the finite element model is based on the experimental work performed by Gesund et al. [30]. A total of twelve simply supported RC beams tested until failure under combined bending and torsion (Figure 1). The cross-section of the beam is 200 mm×200 mm with a 1600 mm clear span length. All beams were reinforced using three bars of tension reinforcement and two bars of compression reinforcement with a 13 mm nominal diameter. Besides, a 10 mm nominal diameter for closed stirrups was applied at 50 mm spacing c-c (Figure 1). The beams were loaded by two-point loads at the end of two-moment arms providing out of plane eccentricity. Hence the beams were subjected to the combined effect of bending and torsion (Figure 1).

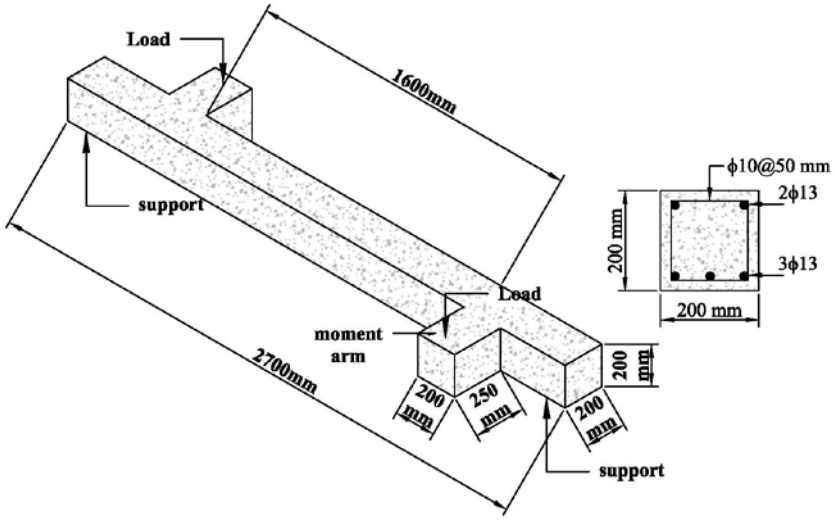

Figure 1. View of the model under load [30].

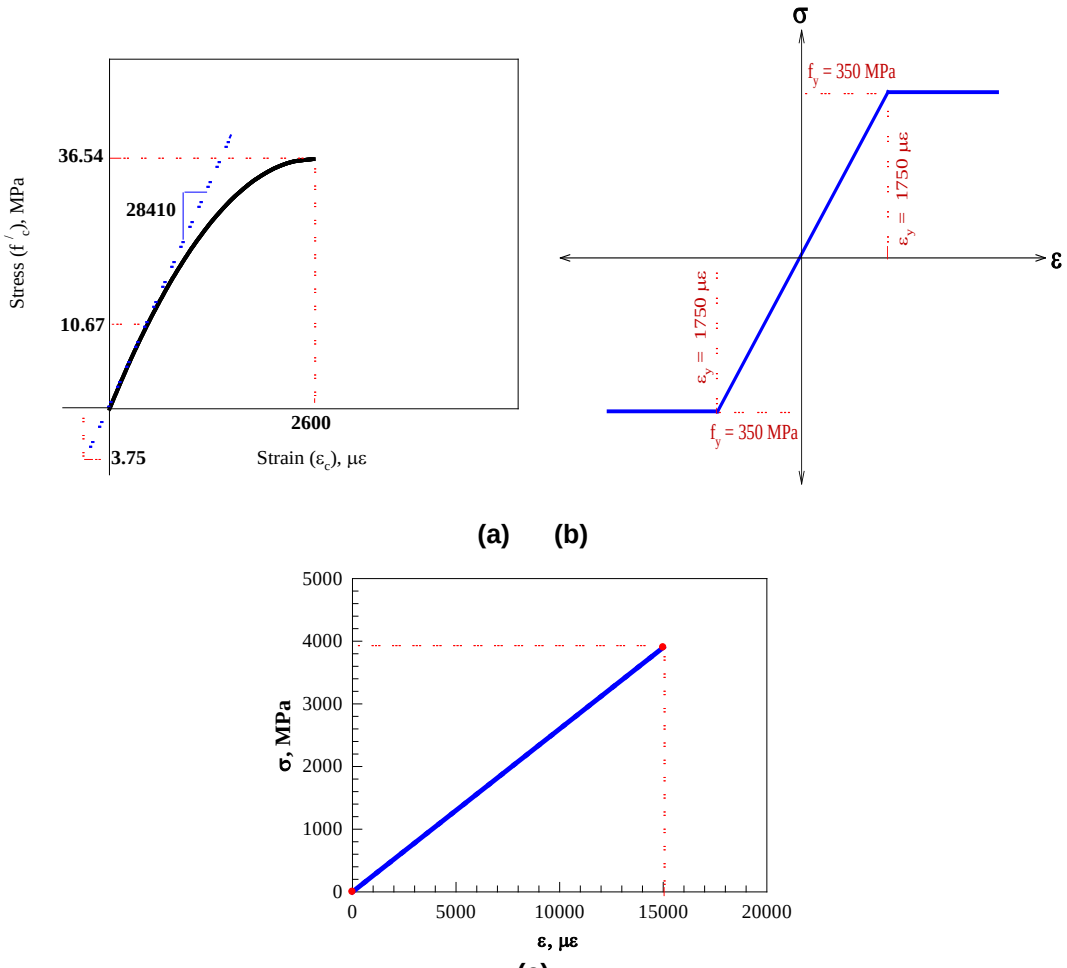

Figure 2. Stress-Strain Curve for (a) Concrete, (b) Steel, and (c) CFRP composite [25].

2.2. Description of Non-linear Finite Element Analysis (NLFEA)

Concrete is a brittle material having high compressive strength compared to tensile strength. The cylindrical compressive strength of concrete is 36.54 MPa. The elastic modulus of elasticity (Ec) and modulus of rupture (fr) of concrete are 28410 MPa and 3.75 MPa, respectively, as shown in Figure 2(a). Concrete poison's ratio is assumed 0.17 for all models. Shear transfer coefficient for open and closed cracks, βt and βc respectively, are important inputs needed for concrete, which indicate the condition of crack surface. In this study, a value of 0.2 and 0.9 is set for the βt and βc, respectively. Steel reinforcement is modeled as a bilinear isotropic material with 200 GPa for the elastic modulus of elasticity and 0.3 of poison's ratio. Its behavior is assumed to be elastic-perfectly plastic, and the same assumption is set for tension and compression reinforcement with yielding stress of 350 MPa, as shown in Figure 2(b). Steel plates are added to the finite element model to avoid stress concentrations at the support and loading locations. These plates are steel type and defined as linear elastic isotropic material with 200 GPa for the elastic modulus of elasticity and 0.3 of poison's ratio. Sika Wrap Hex 300C 0/90 is the CFRP type used in this study. It is a bi-directional material property with 0.166 mm thickness and having fibers in longitudinal and transverse directions. The linear elastic tensile stress-strain curve for CFRP composites is shown in Figure 2(c) and the detailed mechanical properties and poison's ratio in all directions are shown in Table 1.

Table 1. CFRP composites properties.

Modulus of elasticity (GPa)		Poison's ratio		Shear modulus of elasticity (GPa)		Ultimate tensile strength (MPa)	Ultimate strain
E_x	260	V_{xy}	0.22	G_{xy}	106.6	3900	0.015
E_y	260	V_{yz}	0.22	G_{yz}	106.6		
E_z	4.5	V_{zx}	0.30	G_{zx}	1.73		

SOLID 45 is used to model the loading and supporting steel plates. This element is suitable to model the dimensional solid structures defined by eight nodes. There is a presence of translations in the three nodal directions; x, y, and z for each node. SOLID 65 is used to model the concrete which is suitable for tension cracking, crushing in compression and plastic deformations. It is a three-dimensional element defined by eight nodes. Each node has three degrees of freedom with a presence of translations in the three nodal directions; x, y, and z for each node. Steel reinforcement is modeled using link 180, which is a uniaxial tension-compression element. It includes two nodes, and each node has three degrees of freedom. This element can predict large deflection, large strain, rotation, creep, and plasticity. This element can predict large deflection, large strain, stress stiffening, creep, and plasticity. For CFRP, the SHELL 181 element type, having four nodes is used in modeling. It is chosen because it is appropriate to analyze thin layered applications. Three translations and three rotations are considered to include the six degrees of freedom at each node.

The concrete beam and steel plates were modeled as solid elements while steel reinforcement was modeled as link elements. In the case of strengthened RC beams, the CFRP sheets were modeled as shell element with a mesh size of 25 mm. To ensure the perfect bond between concrete and reinforcement, the link element of steel is connected between each adjacent Solid 65 elements, hence the same nodes are shared between the two materials. The same approach is used for the CFRP sheets to provide the perfect bonding as well as for the Steel plates. The geometry of the control and strengthened model, along with the reinforcement specimens are shown in Figure 3(a), Figure 3(b) and Figure 3(c), respectively. The meshing of the CFRP sheet for both fully U wraps and strips wrapping is also shown in Figure 3(d) and Figure 3(e), respectively.

The loads are applied on the two steel plates at the end of the moment arms as line loads distributed over nine nodes. The purpose of these moment arms is to provide the twisting of the main beam. To constrain the model, displacement boundary conditions are required. At the left end of the beam the Ux, Uy, and Uz displacements are set to zero to ensure hinge support. While roller support is added at the right end of the beam by setting zero value to the Uy displacement. Figure 4 shows the loads and boundary conditions of the model. The total applied load is divided into multiple load steps or load increments. Newton–Raphson equilibrium iterations give convergence at the end of each load increment within tolerance limit equal to (0.001) and a load increment of 0.22 kN. When large numbers of cracks appear throughout the concrete, the loads are applied gradually with smaller load increments.

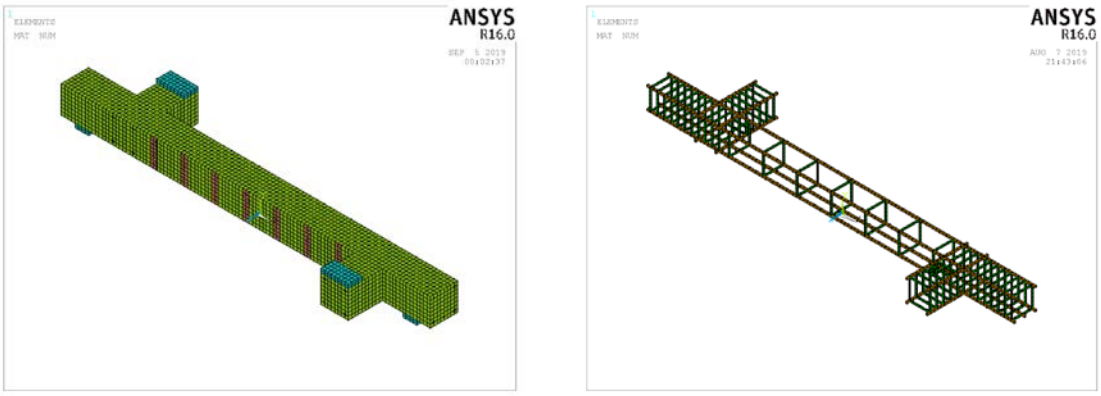

Figure 3. Geometry and meshing.

Table 2. Investigated parameters.

Group number	Beam number	CFRP strengthening configuration	CFRP Anchored Depth (mm)
Control	BC	Control beam without strengthening	0
Group 1	B1	One layer of 50 mm U strip wrapping at 225 mm c/c with an additional layer of CFRP wrapping on both sides of the web	50
	B2		100
	B3		150
	B4		200
Group 2	B5	One layer of 50 mm U strip wrapping at 175 mm c/c with an additional layer of CFRP wrapping on both sides of the web	50
	B6		100
	B7		150
	B8		200
Group 3	B9	One layer of 50 mm U strip wrapping at 125 mm c/c with an additional layer of CFRP wrapping on both sides of the web	50
	B10		100
	B11		150
	B12		200
Group 4	B13	One layer of 50 mm U strip wrapping at 75 mm c/c with an additional layer of CFRP wrapping on both sides of the web	50
	B14		100
	B15		150
	B16		200

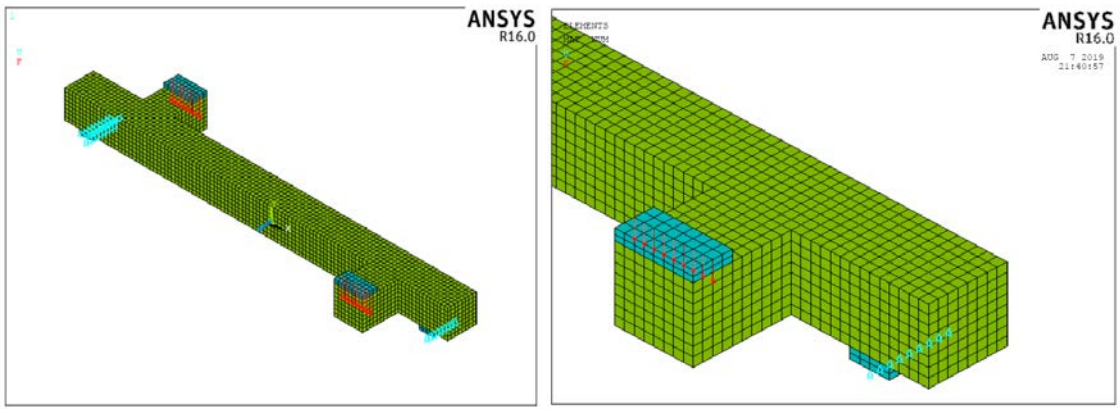

(a) **(b)**

Figure 4. Loads and boundary conditions: (a) 3-D view and (b) Zoomed view.

2.3. Investigated Parameters

Twenty full-scale models strengthened using CFRP are developed to carry out different investigated parameters (Figure 5). A parametric study conducted in this research consists of four groups. The first group contains four models with one layer of 50 mm U strip wrapping at 225 mm c/c with an additional layer of CFRP wrapping on both sides of the web. Group 2 includes four models with one layer of 50 mm U strip wrapping at

175 mm c/c with an additional layer of CFRP wrapping on both sides of the web. The second group includes four models with one layer of 50 mm U strip wrapping at 175 mm c/c with an additional layer of CFRP wrapping on both sides of the web. The third group includes four models with one layer of 50 mm U strip wrapping at 125 mm c/c with an additional layer of CFRP wrapping on both sides of the web. The fourth group includes four models with one layer of 50 mm U strip wrapping at 75 mm c/c with an additional layer of CFRP wrapping on both sides of the web. A full description of the finite element modeling groups is shown in Table 2.

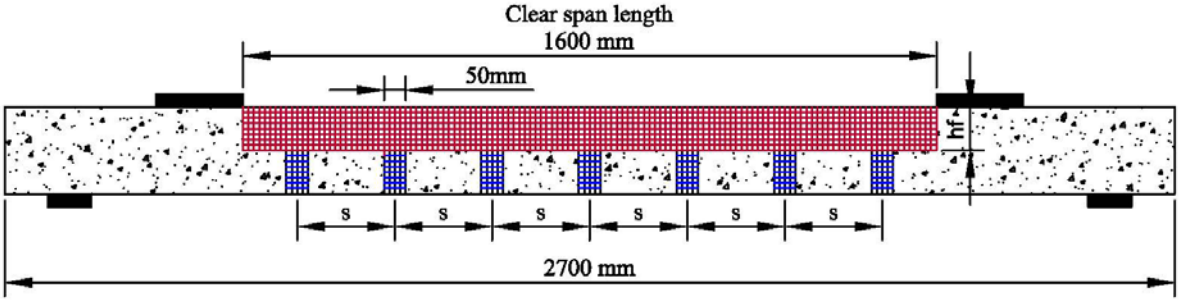

Figure 5. Schematic representation of simulated beams.

2.4. Validation Process

The validation process of the finite element model is based on the experimental work performed by Gesund et al. [30]. Bending and twisting moments at failure as well as the strain in the center bar of longitudinal reinforcement are compared with the NLFEA results. Figure 6 and Table 3 show good agreements between the finite element method and experimental results.

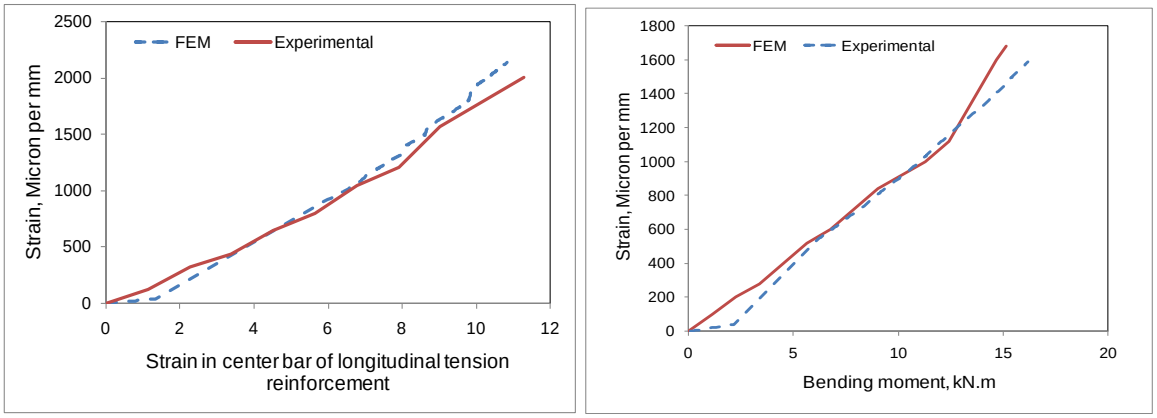

(a) Beam 2 **(b) Beam 4**

Figure 6. Validation of the NLFEA results.

Table 3. Validation summary.

Beam number	Torsion to Bending moment ratio	Bending moment at failure (kN.m)		The torsional moment at failure (kN.m)		Absolute Error %
		Experiment	FEM	Experiment	FEM	
2	1	11.52	10.9	11.52	10.9	5.3
4	0.5	15.14	16.2	7.6	8.1	-6.9

3. Results and Discussion

3.1. Failure Mode

Figure 7 shows the crack pattern for the typically simulated beams. The first crack at an integration point is shown with a red circle outline, the second crack with a green outline, and the third crack with a blue outline. The first crack initiated from the support and then propagated towered the top of the beam in a diagonal shape. Due to the lack of CFRP wrapping along the control beam, this propagation spreads at a faster rate with individual cracks along the beam compared to the strengthened beams. The FRP helps in distribution the stresses on the whole body of the beam. Also, the cracks were smaller and closer to each other, giving higher strength and capacity for those beams. All strengthened beams show almost similar diagonal cracks initiation. This due to the reality of similar loading and boundary conditions and the reinforcement details. However, the fully FRP U- wrap inhibits the propagation of crakes more than FRP strips. The beam strengthened with Fully

FRP U wrap could sustain higher loads and deflections. The failure occurred due to the substantial wide diagonal cracks and concrete crushing followed by FRP failure.

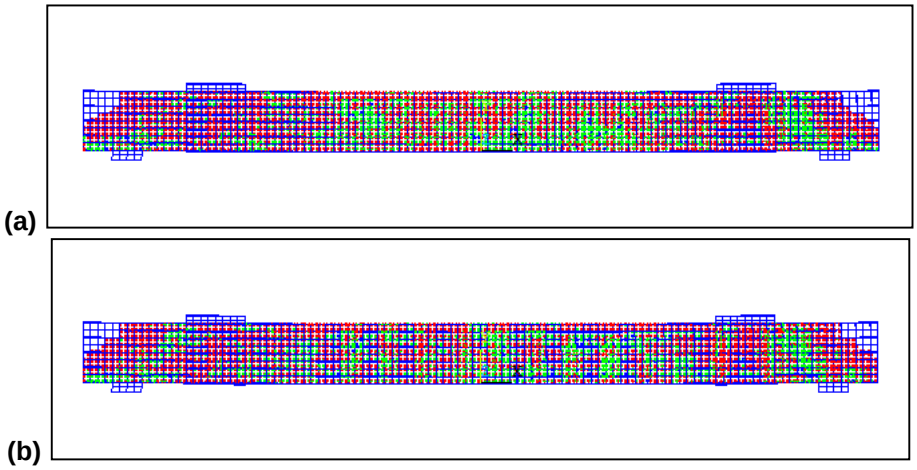

Figure 7. Crack pattern at failure: (a) control beam and (b) strengthened beams using FRP strips.

3.2. CFRP strain

Figure 8 shows the typical distribution of CFRP strain through the depth for all simulated beams. It is noticed that all simulated beams had CFRP strain below the maximum value of 15000 as shown in Table 4 and Table 5 as percentage of CFRP ultimate strain. Inspection of Table 5 reveals that the proposed anchorage system enhanced the efficiency of CFRP strips for Group#1 (S = 225 mm) from 15 % for un-anchored beams to 38 % for beam with anchored depth of 50 mm (hf = 0.25h) and 65% for beam with anchored depth of 200 mm (hf = h). This enhancement percentage increased with the decrease of CFRP strip spacing. The enhancement percentage of anchored system for Group#2 (S =175 mm) is 43% for beam with anchored depth of 50 mm (hf = 0.25h) and 69% for beam with anchored depth of 200 mm (hf = h). Also, the enhancement percentage of anchored system for Group#3 (S =125 mm) is 49% for beam with anchored depth of 50 mm (hf = 0.25h) and 76% for beam with anchored depth of 200 mm (hf = h). Finally, the strip spacing of 75 mm with anchorage enhanced the CFRP strain with a percentage of 54% for beam with anchored depth of 50 mm (hf = 0.25h) and 85% for beam with anchored depth of 200 mm (hf = h).

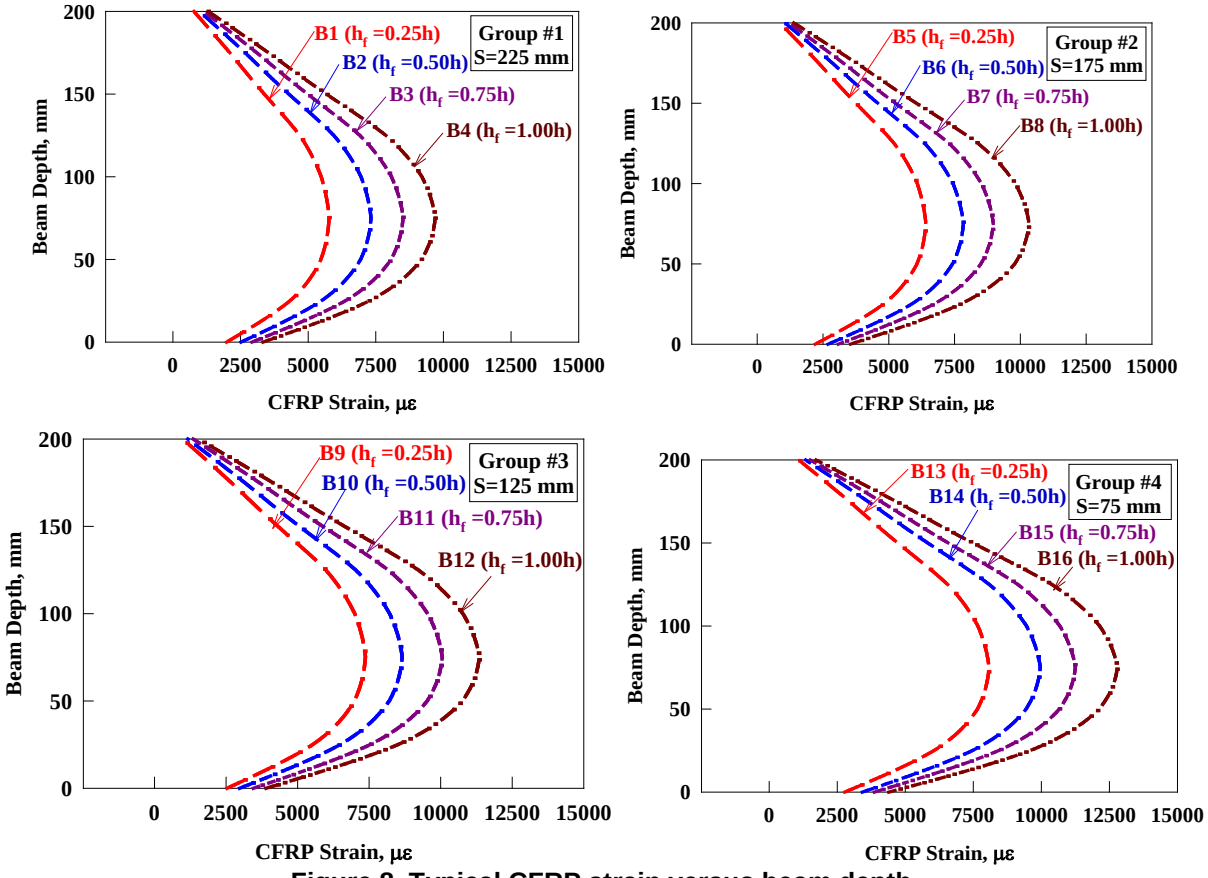

Figure 8. Typical CFRP strain versus beam depth.

3.3. Load-Deflection and Torsion-Twist Behavior

The load-deflection and torsion-twist curves are shown in Figure 9 and 10 respectively. The overall behaviour shown in Figure 9 and 10 indicates that the Anchored CFRP composite provided an increase in the torsional strength and twist at the peak load as well as the ultimate load capacity and corresponding deflection. In general, a linear behaviour before cracking with high torsional stiffness was observed for each strengthened anchored beam, and then the beam suffered an increase in the twist angle with small increasing of torque due to redistribution of forces from the concrete to the steel reinforcement. After this stage and before achieving the peak load, the behaviour became non-linear with a reduction in torsional stiffness.

The strengthened anchored beams exhibited larger twist and deflection at the peak load behaviour in the post-cracking stage due to yielding of the steel reinforcement and possibly slippage of the fibers in the composite. Table 4 illustrates the obtained results for all simulated models. The slope of each region of the load-deflection curves gives the elastic stiffness of the corresponding beam. All strengthened beams represent higher stiffness compared to the control beam in the three regions. Table 4 also shows the calculated energy absorption or area under the load deflection curves for all simulated models.

Table 4. Results for all simulated models.

Group number	Beam number	Ultimate load (kN)	Ultimate deflection (mm)	Ultimate torsion (kN.m)	Ultimate angle of twist (rad)	Elastic stiffness (kN/mm)	Energy absorption (kN.mm2)	CFRP strain (με)
Control	BC	27.8	3.05	0.0132	8.47	3.91	15.3	---
Group 1	B1	34.8	3.63	0.0153	10.62	4.12	22.8	5775
	B2	41.2	4.27	0.0181	12.57	4.14	31.8	7324
	B3	47.2	4.76	0.0210	14.40	4.26	40.6	8510
	B4	54.0	5.25	0.0244	16.45	4.41	51.1	9696
Group 2	B5	31.8	3.83	0.0164	9.70	3.56	22.0	6406
	B6	39.4	4.42	0.0191	12.01	3.82	31.4	7834
	B7	46.0	4.89	0.0217	14.02	4.03	40.6	8972
	B8	53.5	5.45	0.0254	16.32	4.21	52.6	10328
Group 3	B9	36.4	4.08	0.0177	11.09	3.83	26.7	7371
	B10	44.5	4.61	0.0205	13.55	4.14	36.9	8656
	B11	52.4	5.19	0.0234	15.96	4.33	49.0	10055
	B12	61.2	5.72	0.0276	18.65	4.59	63.1	11353
Group 4	B13	39.0	4.22	0.0179	11.90	3.97	29.7	8077
	B14	51.4	4.99	0.0223	15.68	4.42	46.3	9960
	B15	60.7	5.53	0.0259	18.49	4.71	60.5	11250
	B16	71.7	6.16	0.0302	21.85	4.99	79.7	12792

Table 5. Enhancement percentage with respect to control beam.

Group number	Beam number	Ultimate load (%)	Ultimate deflection (%)	Ultimate torsion (%)	Ultimate angle of twist (%)	Elastic stiffness (%)	Energy absorption (%)	ε_{CFRP}
Control	BC	0	0	0	0	0	0	---
Group 1	B1	25	19	25	16	5	49	$0.38\varepsilon_{fu}$
	B2	48	40	48	37	6	108	$0.49\varepsilon_{fu}$
	B3	70	56	70	59	9	165	$0.57\varepsilon_{fu}$
	B4	94	72	94	85	13	234	$0.65\varepsilon_{fu}$
Group 2	B5	44	26	44	24	14	80	$0.43\varepsilon_{fu}$
	B6	78	45	78	44	23	158	$0.52\varepsilon_{fu}$
	B7	107	60	107	64	29	232	$0.60\varepsilon_{fu}$
	B8	141	79	141	93	35	331	$0.69\varepsilon_{fu}$
Group 3	B9	64	34	64	34	23	119	$0.49\varepsilon_{fu}$
	B10	100	51	100	55	33	203	$0.58\varepsilon_{fu}$
	B11	136	70	136	77	39	301	$0.67\varepsilon_{fu}$
	B12	176	88	176	109	47	417	$0.76\varepsilon_{fu}$
Group 4	B13	76	38	76	35	27	143	$0.54\varepsilon_{fu}$
	B14	132	64	132	69	42	280	$0.66\varepsilon_{fu}$
	B15	174	81	174	96	51	396	$0.75\varepsilon_{fu}$
	B16	223	102	223	129	60	553	$0.85\varepsilon_{fu}$

Note: ε_{CFRP} is the strain in CFRP strips and ε_{fu} is the ultimate strain in CFRP strips of 15000 με.

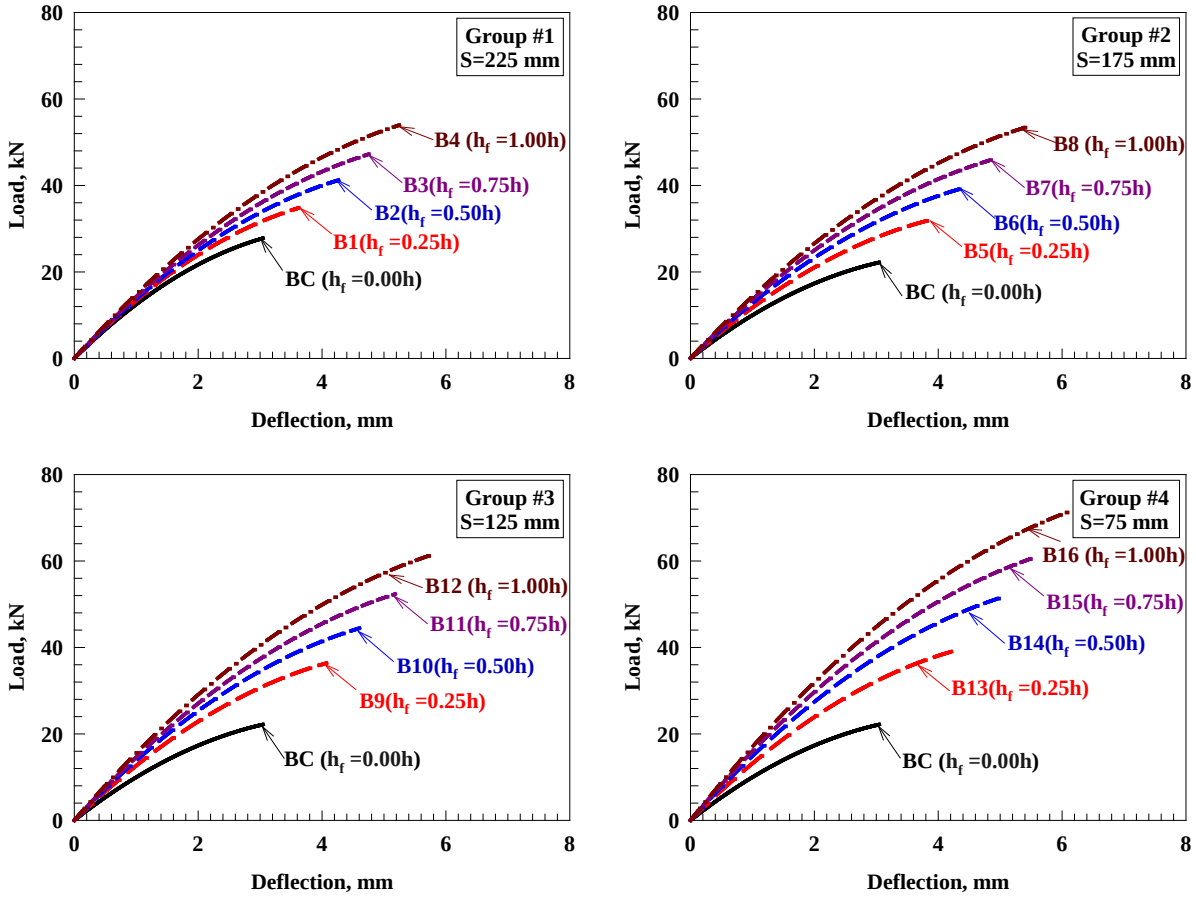

Figure 9. Typical load-deflection curve.

3.4. Ductility and strength ratios

The evaluation of beams for deformability (deflection) and strength (load capacity) shows the superlative performance of RC members. For strengthened RC members, deformability and strength can be related to the serviceability and ultimate load limit states, respectively, of the structural member and can be measured by calculating the strength and ductility ratios, respectively, as shown in Table 5. The strength and ductility ratios are defined as the ultimate load capacity and deflection, respectively, of CFRP strengthened beam divided by the ultimate deflection and load capacity of the un-strengthened beam (control). The ductility indicates how much the strengthened RC beams can sustain deformations without failure. The ductility ratio is defined as the ratio of the ultimate deflection of the strengthened beam to the ultimate deflection of the control beam (Table 5). Strength ratio also predicts the increase of load that the model can sustain.

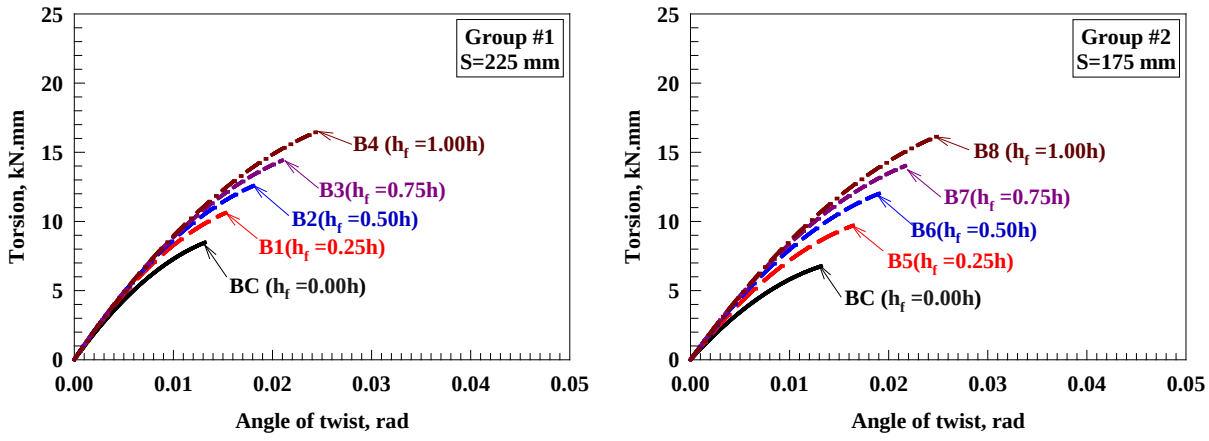

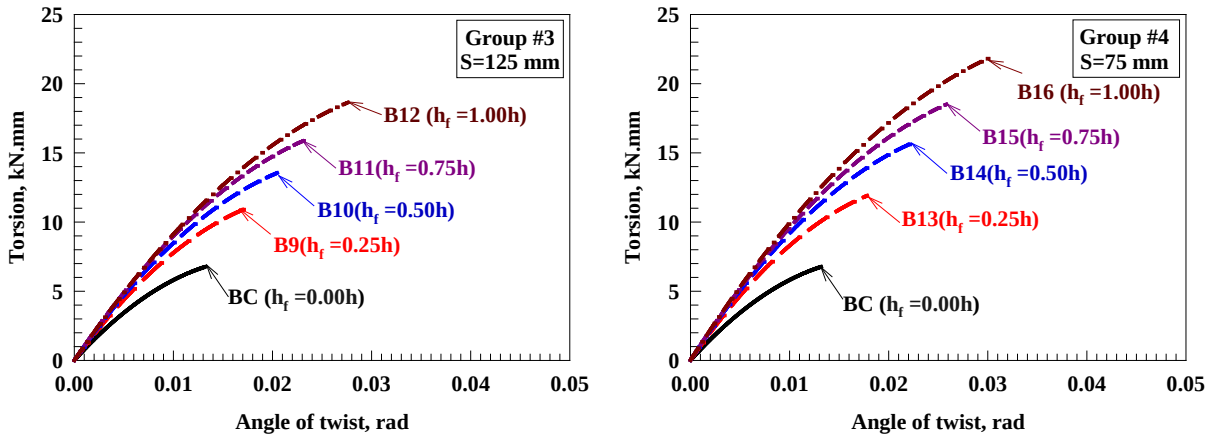

Figure 10. Typical Torsion-angle of twist curve.

Figure 11 and 12 show the strength and ductility ratios, respectively, for all simulated models. Inspection of Figure 11 reveals that the strength ratio enhancement percentage increased largely with the increase of anchored depth (hf) and decreased with the increase of CFRP strip spacing (S). The strength ratio enhancement percentage (Figure 11) for beams strengthened (Group #1) with one layer of 50 mm U strip wrapping at 225 mm c/c with an additional layer of CFRP wrapping on both sides of the web is 25 %, 48 %, 70 %, and 94 % for CFRP anchored depth of 50 mm (hf = 0.25h), 100 (hf = 0.50h) mm, 150 mm (hf = 0.75h), and 200 mm (hf = 1.00h), respectively, with a significant average enhancement of 59 %. Also, the strength ratio enhancement percentage (Figure 11) for beams strengthened (Group #2) with one layer of 50 mm U strip wrapping at 175 mm (equivalent to 78 % of Group #1 spacing) c/c with an additional layer of CFRP wrapping on both sides of the web is 44 %, 78 %, 107 %, and 141 % for CFRP anchored depth of 50 mm (hf = 0.25h), 100 (hf = 0.50h) mm, 150 mm (hf = 0.75h), and 200 mm (hf = 1.00h), respectively, with an significant average enhancement of 93 % and this percentage is 1.56 times the percentage for Group#1 (S = 225 mm). In addition, the strength ratio enhancement percentage (Figure 11) for beams strengthened (Group #3) with one layer of 50 mm U strip wrapping at 125 mm (equivalent to 56 % of Group #1 spacing) c/c with an additional layer of CFRP wrapping on both sides of the web is 64 %, 100 %, 136 %, and 176 % for CFRP anchored depth of 50 mm (hf = 0.25h), 100 (hf = 0.50h) mm, 150 mm (hf = 0.75h), and 200 mm (hf = 1.00h), respectively, with an significant average enhancement of 119% and this percentage is 2 times the percentage for Group#1 (S = 225 mm). While, the Group #4 beams (beams strengthened with one layer of 50 mm U strip wrapping at 75 mm (equivalent to 33 % of Group #1 spacing) c/c with an additional layer of CFRP wrapping on both sides of the web) had the largest average strength ratio enhancement percentage of 151 % and this percentage is 2.55 times the percentage for Group#1 (S = 225 mm). The strength ratio enhancement percentage for beams strengthened (Group #4) is 76%, 132%, 174%, and 223% (Figure 11) for CFRP anchored depth of 50 mm (hf = 0.25h), 100 (hf = 0.50h) mm, 150 mm (hf = 0.75h), and 200 mm (hf = 1.00h), respectively.

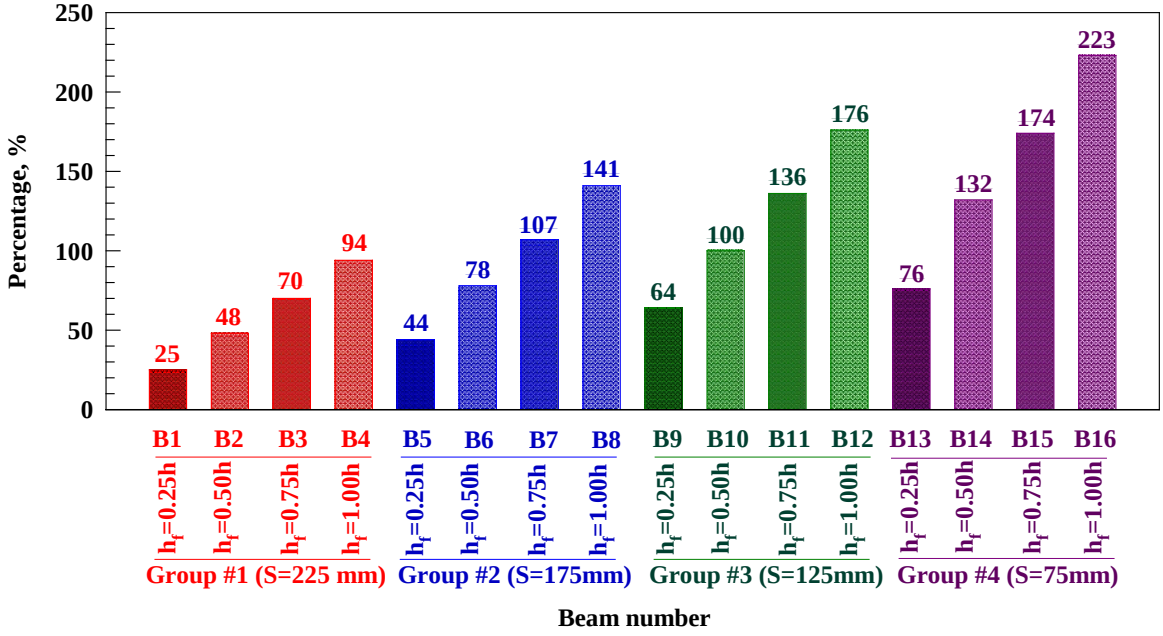

Figure 11. Enhancement percentage in ultimate load capacity (Strength ratio).

Figure 12 shows that the ductility ratio enhancement percentage slightly increased with the increase of hf and decreased with the increase of S. The ductility ratio enhancement percentage (Figure 12) for beams strengthened (Group #1) with one layer of 50 mm U strip wrapping at 225 mm c/c with an additional layer of CFRP wrapping on both sides of the web is 19 %, 40 %, 56 %, and 72 % for CFRP anchored depth of 50 mm (hf = 0.25h), 100 (hf = 0.50h) mm, 150 mm (hf = 0.75h), and 200 mm (hf = 1.00h), respectively, with an significant average enhancement of 47 % (equivalent to 79 % of strength ratio enhancement). Also, the ductility ratio enhancement percentage (Figure 12) for beams strengthened (Group #2) with one layer of 50 mm U strip wrapping at 175 mm (equivalent to 78 % of Group #1 spacing) c/c with an additional layer of CFRP wrapping on both sides of the web is 26 %, 45 %, 60 %, and 79 % for CFRP anchored depth of 50 mm (hf = 0.25h), 100 (hf = 0.50h) mm, 150 mm (hf = 0.75h), and 200 mm (hf = 1.00h), respectively, with an significant average enhancement of 53 % (equivalent to 56 % of strength ratio enhancement) and this percentage is 1.25 times the percentage for Group#1 (S = 225 mm). In addition, the ductility ratio enhancement percentage (Figure 12) for beams strengthened (Group #3) with one layer of 50 mm U strip wrapping at 125 mm (equivalent to 56 % of Group #1 spacing) c/c with an additional layer of CFRP wrapping on both sides of the web is 34 %, 51 %, 70 %, and 88 % for CFRP anchored depth of 50 mm (hf = 0.25h), 100 (hf = 0.50h) mm, 150 mm (hf = 0.75h), and 200 mm (hf = 1.00h), respectively, with an significant average enhancement of 61 % (equivalent to 51 % of strength ratio enhancement) and this percentage is 1.5 times the percentage for Group#1 (S = 225 mm). While, the Group #4 beams (beams strengthened with one layer of 50 mm U strip wrapping at 75 mm (equivalent to 33 % of Group #1 spacing) c/c with an additional layer of CFRP wrapping on both sides of the web) had the largest average ductility ratio enhancement percentage of 71 % (equivalent to 47 % of strength ratio enhancement) and this percentage is 1.75 times the percentage for Group#1 (S = 225 mm). The ductility ratio enhancement percentage for beams strengthened (Group #4) is 38 %, 64 %, 81 %, and 102 % (Figure 12) for CFRP anchored depth of 50 mm (hf = 0.25h), 100 (hf = 0.50h) mm, 150 mm (hf = 0.75h), and 200 mm (hf = 1.00h), respectively.

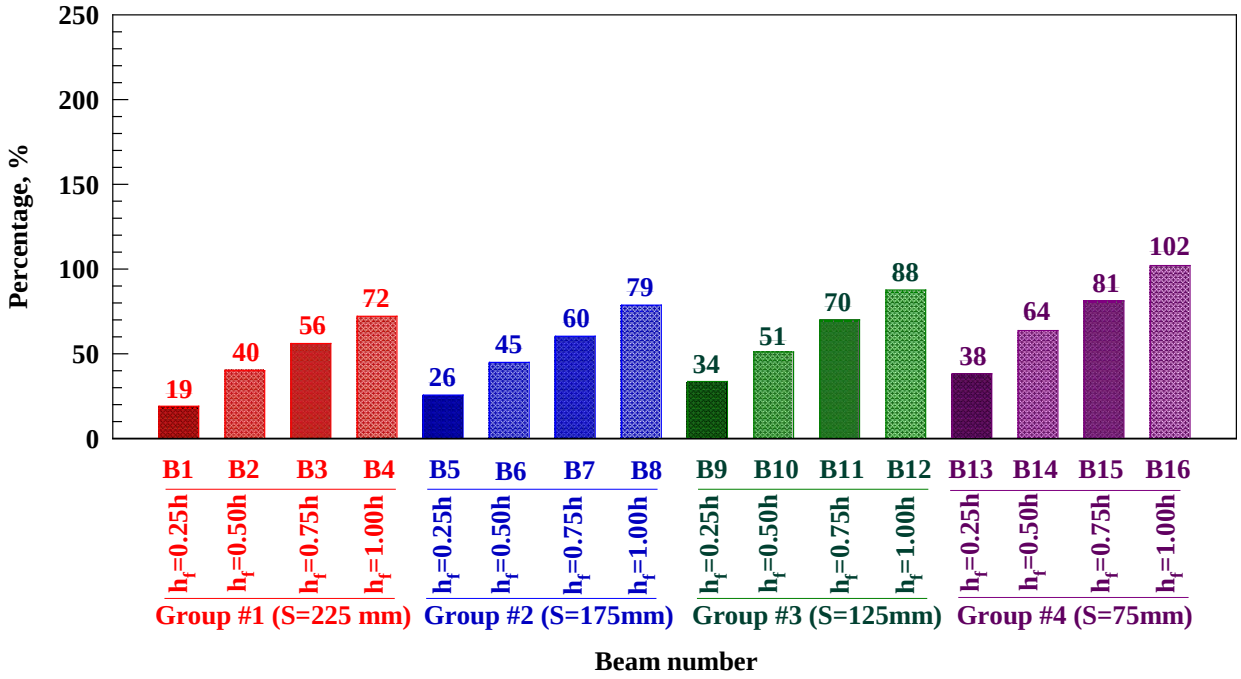

Figure 12. Enhancement percentage in ultimate deflection (ductility ratio).

3.5. Angle of twist ratio

The purpose of a torsion test is to determine the behavior reinforced concrete beam exhibits when twisted or under torsional forces as a result of applied moments that cause shear stress about the axis and angle of twist. The angle of twist can be defined as the angle through which the rotating machine element rotates or twists with respect to its free end as shown in Table 4. Torsional rigidity is the resistance against the torsional deformation or the minimum force required deforming the object by twisting or torsional rigidity is the amount of resistance a cross section has against torsional deformation in terms of twisting angle. Therefore, more angle of twist ratio (Table 5) caused higher torsional rigidity. Figure 13 shows the angle of twist ratio for all simulated models. Inspection of Figure 13 reveals the angle of twist ratio enhancement percentage slightly increased with the increase of hf and decreased with the increase of S.

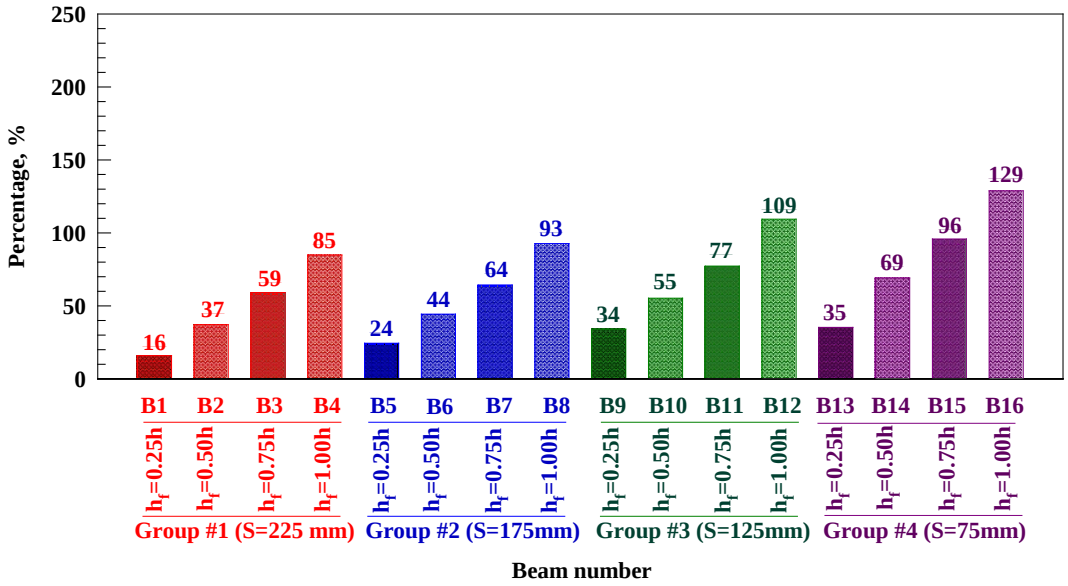

Figure 13. Enhancement percentage in ultimate angle of twist (angle of twist ratio).

The angle of twist ratio enhancement percentage (Figure 13) for beams strengthened (Group #1) with one layer of 50 mm U strip wrapping at 225 mm c/c with an additional layer of CFRP wrapping on both sides of the web is 16 %, 37 %, 59 %, and 85 % for CFRP anchored depth of 50 mm (hf = 0.25h), 100 (hf = 0.50h) mm, 150 mm (hf = 0.75h), and 200 mm (hf = 1.00h), respectively, with an significant average enhancement of 49 % (equivalent to 105 % of ductility ratio enhancement). Also, the angle of twist ratio enhancement percentage (Figure 13) for beams strengthened (Group #2) with one layer of 50 mm U strip wrapping at 175 mm (equivalent to 78 % of Group #1 spacing) c/c with an additional layer of CFRP wrapping on both sides of the web is 24 %, 44 %, 64 %, and 93 % for CFRP anchored depth of 50 mm (hf = 0.25h), 100 (hf = 0.50h) mm, 150 mm (hf = 0.75h), and 200 mm (hf = 1.00h), respectively, with an significant average enhancement of 56 % (equivalent to 108 % of ductility ratio enhancement) and this percentage is 1.15 times the percentage for Group#1 (S = 225 mm). In addition, the angle of twist ratio enhancement percentage (Figure 13) for beams strengthened (Group #3) with one layer of 50 mm U strip wrapping at 125 mm (equivalent to 56 % of Group #1 spacing) c/c with an additional layer of CFRP wrapping on both sides of the web is 34 %, 55 %, 77 %, and 109 % for CFRP anchored depth of 50 mm (hf = 0.25h), 100 (hf = 0.50h) mm, 150 mm (hf = 0.75h), and 200 mm (hf = 1.00h), respectively, with an significant average enhancement of 69 % (equivalent to 114 % of ductility ratio enhancement) and this percentage is 1.4 times the percentage for Group#1 (S = 225 mm). While, the Group #4 beams (beams strengthened with one layer of 50 mm U strip wrapping at 75 mm (equivalent to 33 % of Group #1 spacing) c/c with an additional layer of CFRP wrapping on both sides of the web) had the largest average angle of twist ratio enhancement percentage of 72 % (equivalent to 115 % of ductility ratio enhancement) and this percentage is 1.67 times the percentage for Group#1 (S = 225 mm). The angle of twist ratio enhancement percentage for beams strengthened (Group #4) is 35 %, 69 %, 96 %, and 129 % (Figure 13) for CFRP anchored depth of 50 mm (hf = 0.25h), 100 (hf = 0.50h) mm, 150 mm (hf = 0.75h), and 200 mm (hf = 1.00h), respectively.

3.6. Elastic stiffness ratio

The elastic stiffness determines the response of the crystal to an externally applied strain (or stress) and provides information about the bonding characteristics, mechanical and structural stability. The slope of the first stage of the load-deflection curve before initiation of the first main flexural crack is represented the elastic stiffness. For comparison, the elastic stiffness of each strengthened beam with CFRP sheets was normalized with respect to the control beams without CFRP sheets as shown in Table 5.

Figure 14 shows the elastic stiffness ratio for all simulated models. Inspection of Figure 14 reveals the elastic stiffness ratio enhancement percentage is classified as the least percentage in the investigated parameters in this study in which slightly increased with the increase of hf and decreased with the increase of S. The elastic stiffness ratio enhancement percentage (Figure 14) for beams strengthened (Group #1) with one layer of 50 mm U strip wrapping at 225 mm c/c with an additional layer of CFRP wrapping on both sides of the web is 5 %, 6 %, 9 %, and 13 % for CFRP anchored depth of 50 mm (hf = 0.25h), 100 (hf = 0.50h) mm, 150 mm (hf = 0.75h), and 200 mm (hf = 1.00h), respectively, with a small average enhancement of 8 % (equivalent to 18 % of ductility ratio enhancement). Also, the elastic stiffness ratio enhancement percentage (Figure 14) for beams strengthened (Group #2) with one layer of 50 mm U strip wrapping at 175 mm (equivalent to 78 % of Group #1 spacing) c/c with an additional layer of CFRP wrapping on both sides of the web is 14 %, 23 %, 29 %, and 35 % for CFRP anchored depth of 50 mm (hf = 0.25h), 100 (hf = 0.50h) mm, 150 mm (hf = 0.75h), and 200 mm (hf = 1.00h), respectively, with a small average enhancement of 25 % (equivalent to 48 % of ductility ratio enhancement) and this percentage is 3.1 times the percentage for Group#1

(S = 225 mm). In addition, the elastic stiffness ratio enhancement percentage (Figure 14) for beams strengthened (Group #3) with one layer of 50 mm U strip wrapping at 125 mm (equivalent to 56 % of Group #1 spacing) c/c with an additional layer of CFRP wrapping on both sides of the web is 23 %, 33 %, 39 %, and 47 % for CFRP anchored depth of 50 mm (hf = 0.25h), 100 (hf = 0.50h) mm, 150 mm (hf = 0.75h), and 200 mm (hf = 1.00h), respectively, with a small average enhancement of 35 % (equivalent to 58 % of ductility ratio enhancement) and this percentage is 4.3 times the percentage for Group#1 (S = 225 mm). While, the Group #4 beams (beams strengthened with one layer of 50 mm U strip wrapping at 75 mm (equivalent to 33 % of Group #1 spacing) c/c with an additional layer of CFRP wrapping on both sides of the web) had the largest average elastic stiffness ratio enhancement percentage of 45 % (equivalent to 63 % of ductility ratio enhancement) and this percentage is 5.5 times the percentage for Group#1 (S = 225 mm). The elastic stiffness ratio enhancement percentage for beams strengthened (Group #4) is 27 %, 42 %, 51 %, and 60 % (Figure 14) for CFRP anchored depth of 50 mm (hf = 0.25h), 100 (hf = 0.50h) mm, 150 mm (hf = 0.75h), and 200 mm (hf = 1.00h), respectively.

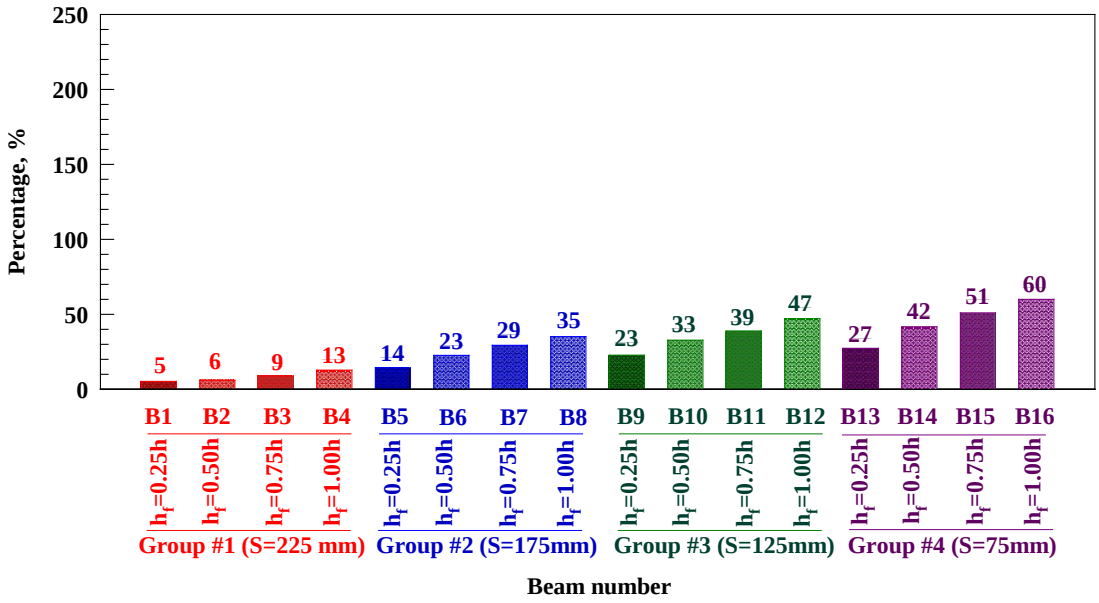

Figure 14. Enhancement percentage in elastic stiffness (elastic stiffness ratio).

3.7. Energy absorption ratio

In materials science and metallurgy, energy absorption or toughness is the ability of a material to absorb energy and plastically deform without fracturing. One definition of material toughness is the amount of energy per unit volume that a material can absorb before rupturing. Energy absorption is calculated as the entire area under the load-deflection curve. In addition, the energy absorption of each strengthened beam with CFRP sheets was normalized with respect to the control beams without CFRP sheets as shown in Table 5.

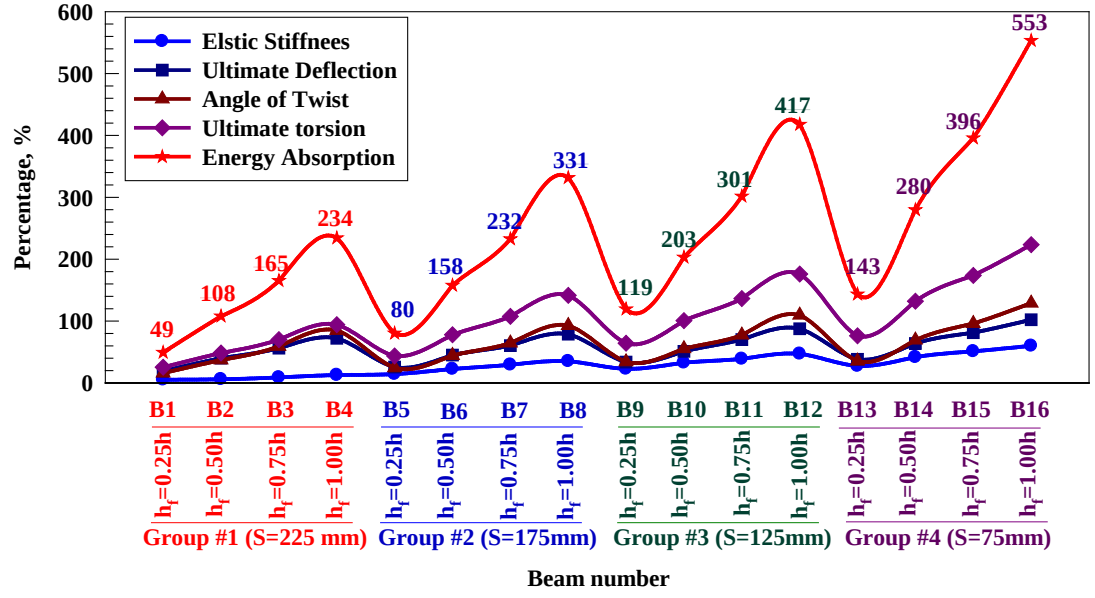

Figure 15. Enhancement percentage in energy absorption (energy absorption ratio).

Figure 15 shows the energy absorption ratio for all simulated models. Inspection of Figure 15 reveals the energy absorption ratio enhancement percentage is classified as the highest percentage in the investigated parameters in this study in which largely increased with the increase of hf and decreased with the increase of S. The energy absorption ratio enhancement percentage (Figure 15) for beams strengthened (Group #1) with one layer of 50 mm U strip wrapping at 225 mm c/c with an additional layer of CFRP wrapping on both sides of the web is 49 %, 108 %, 165 %, and 234 % for CFRP anchored depth of 50 mm (hf = 0.25h), 100 (hf = 0.50h) mm, 150 mm (hf = 0.75h), and 200 mm (hf = 1.00h), respectively, with enormous average enhancement of 139 % (equivalent to 1692 % of elastic stiffness ratio enhancement). Also, the energy absorption ratio enhancement percentage (Figure 15) for beams strengthened (Group #2) with one layer of 50 mm U strip wrapping at 175 mm (equivalent to 78 % of Group #1 spacing) c/c with an additional layer of CFRP wrapping on both sides of the web is 80 %, 158 %, 232 %, and 331 % for CFRP anchored depth of 50 mm (hf = 0.25h), 100 (hf = 0.50h) mm, 150 mm (hf = 0.75h), and 200 mm (hf = 1.00h), respectively, with enormous average enhancement of 200 % (equivalent to 2438 % of elastic stiffness ratio enhancement) and this percentage is 1.44 times the percentage for Group#1 (S = 225 mm). In addition, the energy absorption ratio enhancement percentage (Figure 15) for beams strengthened (Group #3) with one layer of 50 mm U strip wrapping at 125 mm (equivalent to 56 % of Group #1 spacing) c/c with an additional layer of CFRP wrapping on both sides of the web is 119 %, 203 %, 301 %, and 417 % for CFRP anchored depth of 50 mm (hf = 0.25h), 100 (hf = 0.50h) mm, 150 mm (hf = 0.75h), and 200 mm (hf = 1.00h), respectively, with enormous average enhancement of 260 % (equivalent to 3166 % of elastic stiffness ratio enhancement) and this percentage is 1.87 times the percentage for Group#1 (S = 225 mm). While, the Group #4 beams (beams strengthened with one layer of 50 mm U strip wrapping at 75 mm (equivalent to 33 % of Group #1 spacing) c/c with an additional layer of CFRP wrapping on both sides of the web) had the largest average energy absorption ratio enhancement percentage of 343 % (equivalent to 4172 % of elastic stiffness ratio enhancement) and this percentage is 2.4 times the percentage for Group#1 (S = 225 mm). The energy absorption ratio enhancement percentage for beams strengthened (Group #4) is 143 %, 280 %, 393 %, and 553 % (Figure 14) for CFRP anchored depth of 50 mm (hf = 0.25h), 100 (hf = 0.50h) mm, 150 mm (hf = 0.75h), and 200 mm (hf = 1.00h), respectively.

3.8. Comparison of NLFEA with other results

Comparison of NLFEA with Vishnu et al. [31], the bending moment and torque for all specimens at first crack are closed to NLFEA. Due to FRP torsional resistance of beam is increased in all types of wrapping configuration. Maximum bending moment and torsional moment are resisted by FRP strengthening. Also, all specimens wrapped with GFRP show better torsional resistance compared to the control specimen. Results show an increase in structural behavior of the strengthened beam is almost the same performance as the NLFEA. Besides, Vishnu et al. [31] reached the same conclusion as NLFEA that the fully U wrap strengthening technique of RC beam with FRP is more efficient in resisting torsional moment compared to the vertical strip.

4. Conclusions

1. Integration of CFRP strips as anchored external shear CFRP strips in RC beams can be conducted with alleviate, which eliminates the need for decreasing the center to center spacing between CFRP strips.

2. The control beam shows a faster rate of diagonal crack propagation than the strengthened beams. This is due to the lack of CFRP wrapping along the beam. The failure occurred after substantial wide diagonal cracks and concrete crushing followed by CFRP rupture.

3. The using of anchored CFRP sheets along the top face of the beam as external strengthening in the enhancing of the beam shear integrity pre and post cracking, arresting the shear cracks and improving the structural performance and serviceability of simulated beam.

4. The efficiency of using CFRP strips increases as decreasing the center to center spacing between CFRP strips. For the same spacing, this efficiency increases as increasing the depth of anchored CFRP.

5. The external strengthening with anchored had a superior effect on the CFRP strain (15%–85%), ultimate load (25%–223%), ultimate deflection (19%–102%), angle of twist (16%–129%), torsion elastic stiffness (5%–60%), energy absorption (49%–553%).

6. The enhancement percentage increased with the increase of anchored depth and decreased with the increase of CFRP strip spacing.

References

1. Saadatmanesh, H., Ehsani, M. RC Beams Strengthened with GFRP Plates. I: Experimental Study. Journal of Structural Engineering. 1991.117(1). Pp. 3417–3433. DOI: 10.1061/(ASCE)0733-9445(1991)117:11(3417)
2. Wei, A., Saadatmanesh, H., Ehsani, M. RC Beams Strengthened with FRP Plates. II: Analysis and Parametric Study. Journal of Structural Engineering. 1991. 117(1). Pp. 3434–3455. DOI: 10.1061/(ASCE)0733-9445(1991)117:11(3434)
3. Chen, J., Teng, J. Shear capacity of fiber-reinforced polymer-strengthened reinforced concrete beams: fiber reinforced polymer rupture. Journal of Structural Engineering. 2003.129(1). Pp. 615–625. DOI: 10.1061/(ASCE)0733-9445(2003)129:5(615)

4. Chen, J.-F., Teng, J.-G. Shear capacity of FRP-strengthened RC beams: FRP debonding. Construction and Building Materials. 2003.17(1). Pp. 27–41. DOI: 10.1016/S0950-0618(02)00091-0
5. Volkova, A., Rybakov, V., Seliverstov, A., Petrov, D., Smignov, A. Lightweight steel concrete structures slab panels load-bearing capacity. MATEC Web of Conferences. 2018. 245. 08007. doi.org/10.1051/matecconf/201824508008
6. Vatin, N.I., Velichkin, V.Z., Kozinetc, G.L., Korsun, V.I., Rybakov, V.A., Zhuvak, O.V. Precast-monolithic reinforced concrete beam-slabs technology with claydit blocks. Construction of Unique Buildings and Structures. 2018. 70(7). Pp. 43–59. DOI: 10.18720/CUBS.70.4
7. Rybakov, V.A., Kozinetc, K.G., Vatin, N.I., Velichkin, V.Z., Korsun, V.I. Lightweight steel concrete structures technology with foam fiber-cement sheets. Magazine of Civil Engineering. 2018. 82(6). Pp. 103–111. DOI: 10.18720/MCE.82.10
8. Shen, K., Wan, S., Mo, Y.L., Jiang, Z. Theoretical analysis on full torsional behavior of RC beams strengthened with FRP materials. Composite Structures. 2018. 183(1). Pp. 347–357. DOI: 10.1016/j.compstruct.2017.03.084.
9. Jariwala, V.H., Patel, P., Purohit, S.P. Strengthening of RC beams subjected to combined torsion and bending with GFRP composites. Procedia Engineering. 2013. 51(1). Pp. 282–289. DOI: 10.1016/j.proeng.2013.01.038
10. Amulu, C.P., Zeagu, C.A. Experimental and analytical comparison of torsion, bending moment and shear forces in reinforced concrete beams using BS 8110, euro code 2 and ACI 318 provisions. Nigerian Journal of Technology. 2017. 36(3). Pp. 705–711. DOI: 10.4314/njt.v36i3.7.
11. Alabdulhady, M.Y., Sneed, L.H., Carloni, C. Torsional behavior of RC beams strengthened with PBO-FRCM composite–An experimental study. Engineering Structures. 2017. 136(1). Pp. 393–405. DOI: 10.1016/j.engstruct.2017.01.044
12. Ameli, M., Ronagh, H.R., Dux, P.F. Behavior of FRP strengthened reinforced concrete beams under torsion. Journal of Composites for Construction. 2007. 11(1). Pp.192–200. DOI: 10.1061/(ASCE)1090-0268(2007)11:2(192)
13. Chalioris, C.E. Tests and analysis of reinforced concrete beams under torsion retrofitted with FRP strips. Computational Methods and Experimental Measurements XIII. 2007. 46(1). Pp. 633–642. DOI: 10.2495/CMEM070631
14. Hii, A.K.Y., Al-Mahaidi, R. Experimental investigation on torsional behavior of solid and box-section RC beams strengthened with CFRP using photogrammetry. Journal of Composites for Construction. 2006. 10(1). Pp. 321–329. DOI: 10.1061/(ASCE)1090-0268(2006)10:4(321)
15. Jing, M., Raongjant, W., Li, Z. Torsional strengthening of reinforced concrete box beams using carbon fiber reinforced polymer. Composite Structures 2007. 78(1). Pp. 264–270. DOI: 10.1016/j.compstruct.2005.10.017
16. Chalioris, C.E. Torsional strengthening of rectangular and flanged beams using carbon fibre-reinforced-polymers–experimental study. Construction and Building Materials. 2008. 22(1). Pp. 21–29. DOI: 10.1016/j.conbuildmat.2006.09.003
17. Deifalla, A., Ghobarah, A. Strengthening RC T-beams subjected to combined torsion and shear using FRP fabrics: experimental study. Journal of Composites for Construction. 2010. 14(1). Pp. 301–311. DOI: 10.1061/(ASCE)CC.1943-5614.0000091
18. Salom, P.R., Gergely, J., Young, D.T. Torsional strengthening of spandrel beams with fiber-reinforced polymer laminates. Journal of Composites for Construction. 2004. 8(1). Pp. 157–162. DOI: 10.1061/(ASCE)1090-0268(2004)8:2(157)
19. He, R., Sneed, L.H., Belarbi, A. Torsional repair of severely damaged column using carbon fiber-reinforced polymer. Aci Structural Journal. 2014.111(1). Pp. 705–716. DOI: 10.14359/51686627
20. Yang, Y., Sneed, L., Saiidi, M.S., Belarbi, A., Ehsani, M., He, R. Emergency repair of an RC bridge column with fractured bars using externally bonded prefabricated thin CFRP laminates and CFRP strips. Composite Structures 2015. 133(1). Pp. 727–738. DOI: 10.1016/j.compstruct.2015.07.045
21. Gonzalez-Libreros, J.H., Sneed, L.H., D'Antino, T., Pellegrino, C. Behavior of RC beams strengthened in shear with FRP and FRCM composites. Engineering Structures. 2017. 150(1). Pp. 830–842. DOI: 10.1016/j.engstruct.2017.07.084.
22. Ghobarah, A., Ghorbel, M.N., Chidiac, S.E. Upgrading torsional resistance of reinforced concrete beams using fiber-reinforced polymer. Journal of Composites for Construction. 2002. 6(1). Pp. 257–263. DOI: 10.1061/(ASCE)1090-0268(2002)6:4(257)
23. Hii, A.K.Y., Al-Mahaidi, R. An experimental and numerical investigation on torsional strengthening of solid and box-section RC beams using CFRP laminates. Composite Structures. 2006. 75(1). Pp. 213–221. DOI: doi.org/10.1016/j.compstruct.2006.04.050
24. Ganganagoudar, A., Mondal, T.G., Suriya Prakash, S. Analytical and finite element studies on behavior of FRP strengthened RC beams under torsion. Composite Structures. 2016. 153(1). Pp. 876–885. DOI: 10.1016/j.compstruct.2016.07.014
25. Al-Rousan, R., Abo-Msamh, I. Bending and Torsion Behaviour of CFRP Strengthened RC Beams. Magazine of Civil Engineering. 2019. 92(8). Pp. 62–71. DOI: 10.18720/MCE.92.8
26. Mahmood, M.N. Nonlinear analysis of reinforced concrete beams under pure torsion. Journal of Applied Sciences. 2007. 7(22). Pp. 3524–3529. DOI: 10.3923/jas.2007.3524.3529
27. Prabaghar, A., Kumaran, G. Theoretical study on the behavior of rectangular concrete beams reinforced internally with GFRP reinforcements under pure torsion. International Journal of Civil and Structural Engineering. 2011. 2(2). Pp. 570–594. DOI: 10.6088/ijcser.00202010134.
28. Elwan, S.K. Torsion strengthening of RC beams using CFRP (parametric study). Journal of Civil Engineering. 2017. 21(4). Pp. 1273–1281. DOI: 10.1007/s12205-016-0156-7.
29. Zojaji, A.R., Kabir, M.Z. Analytical approach for predicting full torsional behavior of reinforced concrete beams strengthened with FRP materials. Scientia Iranica. 2012. 19(2). Pp. 51-63. DOI: 10.1016/j.scient.2011.12.004.
30. Gesund, H., Schuette, F.J., Buchanan, G.R., Gray, G.A. Ultimate strength in combined bending and torsion of concrete beams containing both longitudinal and transverse reinforcement. Journal of the American Concrete Institute. 1964. 61(12). Pp. 1509–1522. DOI: 10.1680/macr.1968.20.64.155.
31. Jariwala, V.H., Patel, P.V., Purohit, S.P. Strengthening of RC Beams Subjected to Combined Torsion and Bending with GFRP Composites. Procedia Engineering. 2013. 51(1). Pp. 282-289. DOI: 10.1016/j.proeng.2013.01.038

Contacts:

Rajai Al-Rousan, rzalrousan@just.edu.jo
Isra'a Abo-Msamh, iabomsamh@gmail.com